Achieving λ/20 Resolution by One-Color Initiation and Deactivation of Polymerization

Linjie Li, *et al.*

Science **324**, 910 (2009);
DOI: 10.1126/science.1168996

Achieving λ/20 Resolution by One-Color Initiation and Deactivation of Polymerization

Linjie Li,[1] Rafael R. Gattass,[1] Erez Gershgoren,[1] Hana Hwang,[2] John T. Fourkas[1,3,4,5]*

In conventional photolithography, diffraction limits the resolution to about one-quarter of the wavelength of the light used. We introduce an approach to photolithography in which multiphoton absorption of pulsed 800-nanometer (nm) light is used to initiate cross-linking in a polymer photoresist and one-photon absorption of continuous-wave 800-nm light is used simultaneously to deactivate the photopolymerization. By employing spatial phase-shaping of the deactivation beam, we demonstrate the fabrication of features with scalable resolution along the beam axis, down to a 40-nm minimum feature size. We anticipate application of this technique for the fabrication of diverse two- and three-dimensional structures with a feature size that is a small fraction of the wavelength of the light employed.

The demand for increasingly powerful integrated circuits has spurred remarkable progress in lithographic techniques in the past decades (*1*). However, progress toward higher resolution has proven to be increasingly difficult and expensive as feature sizes decrease. To improve resolution in photolithography, chemical nonlinearity can be employed to create a sharp intensity threshold for exposure (*2*). However, diffractive effects still limit feature sizes in conventional photolithography to about a quarter of a wavelength (λ) of the light used to expose the photoresist.

Nonlinear optical phenomena provide an alternative approach to photolithography (*3*–*6*). In multiphoton absorption polymerization (MAP), a photoinitiator in a prepolymer resin is excited by the simultaneous absorption of two or more photons of light. The absorption probability depends on the laser intensity to the power of the number of photons needed to cause an electronic transition, so an ultrafast laser is generally used to provide high peak intensity at low average power. The laser is focused through a microscope objective such that the intensity of the light is only high enough to drive multiphoton absorption in the small region defined by the focal volume of the beam. In the most common implementation of MAP, multiphoton absorption initiates cross-linking that hardens the prepolymer resin within the focal volume. By moving this focal volume relative to the sample, complex, three-dimensional (3D) polymeric structures can be created.

Due to the optical nonlinearity of multiphoton absorption and the existence of an intensity threshold for polymerization, MAP can be used to create volume elements (voxels) with a resolution that is considerably smaller than the wavelength of the light used. For instance, 800 nm light has been used with MAP to create voxels with a transverse dimension of 80 nm (*7*), corresponding to λ/10 resolution. Even finer resolution has been reported for suspended lines, although based on the tapered nature of these lines at their attachment points, it is likely that shrinkage during the developing stage plays a role in this case (*8*). Using light of a shorter wavelength for MAP can also improve resolution (*9*). It should be noted that because of the shape of the focal region of the laser beam, the resolution of MAP along the beam axis is usually poorer by a factor of at least three than the transverse resolution (*10*).

We used a technique that we call resolution augmentation through photo-induced deactivation (RAPID) lithography. In RAPID lithography, one laser beam is used to initiate polymerization in a negative-tone photoresist. A second laser beam is used to deactivate the photoinitiator, preventing photopolymerization from occurring. By spatial shaping of the phase of the deactivation beam, features far smaller than the excitation wavelength can be fabricated.

The inspiration for RAPID lithography comes from stimulated emission depletion (STED) fluorescence microscopy (*11*–*13*). In STED, fluorescent molecules are excited by a short laser pulse. A second laser pulse, which is tuned to a substantially longer wavelength than the first pulse, is used to de-excite the molecules through stimulated emission. This depletion pulse must arrive after vibrational relaxation is complete in the excited electronic state but before significant fluorescence has occurred. Spatial phase shaping of the depletion beam causes de-excitation to occur everywhere except in a region at the center of the original focal volume (*11*–*13*). The size of this region depends on the intensity of the depletion beam and the corresponding degree of saturation of stimulated emission. Thus, fluorescence can be localized in a zone much smaller than the excitation wavelength.

In principle, STED should work equally well to deactivate polymerization in MAP or even

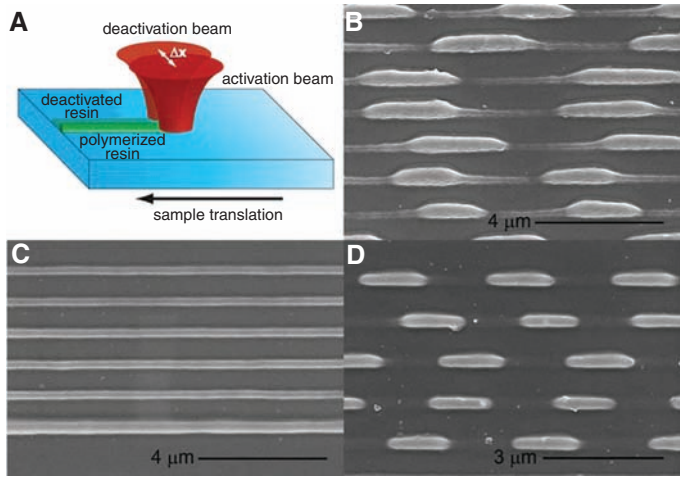

Fig. 1. (**A**) Schematic illustration of the experimental setup for demonstrating photoinduced deactivation of photopolymerization. The excitation and deactivation beams are focused in the prepolymer resin with a lateral separation of Δx. The substrate is translated perpendicular to the separation axis to fabricate polymer lines. (**B**) Top-view scanning electron micrograph of lines written with offset ($\Delta x > 0$), 200-fs excitation pulses and 50-ps deactivation pulses. The deactivation beam was chopped. The excitation power was 7 mW and the deactivation power 70 mW. (**C**) Top-view SEM of lines written with different timings between the excitation and deactivation pulses. The deactivation beam was at a low enough power to inhibit polymerization incompletely. The bottom line was written without a deactivation beam, and the remaining lines were written with delay times, from bottom to top, of 7 ns, 12 ns, 0 ns, 1 ns, and 6 ns; all delay uncertainties are <1 ps. The excitation power was 7 mW and the deactivation power 50 mW. (**D**) Top-view SEM of lines written with coincident ($\Delta x = 0$), 200-fs excitation pulses and a CW deactivation beam that was chopped to turn polymerization off and on. The excitation power was 5 mW and the deactivation power 34 mW.

[1]Department of Chemistry and Biochemistry, University of Maryland, College Park, MD 20742, USA. [2]Department of Physics, University of Maryland, College Park, MD 20742, USA. [3]Institute for Physical Science and Technology, University of Maryland, College Park, MD 20742, USA. [4]Maryland NanoCenter, University of Maryland, College Park, MD 20742, USA. [5]Center for Nanophysics and Advanced Materials, University of Maryland, College Park, MD 20742, USA.

*To whom correspondence should be addressed. E-mail: fourkas@umd.edu

conventional photopolymerization. Typical radical photoinitiators undergo intersystem crossing to a triplet state on a time scale on the order of 100 ps (*14*). The radicals that lead to polymerization are formed in the triplet state, so de-excitation of molecules before intersystem crossing occurs will turn off photopolymerization. Furthermore, radical photopolymerization only occurs above a threshold concentration of radicals, so de-excitation of a small fraction of excited photoinitiator molecules could be sufficient to halt polymerization if the concentration of excited molecules is just above this threshold. In practice, to achieve efficient de-excitation, stimulated emission must dominate over absorption from the first excited electronic state to higher excited states, which will only happen when the oscillator strength between the ground and first excited electronic states is large (*15*). This oscillator strength condition is met for the strongly fluorescent molecules used for STED. However, radical photoinitiators generally have relatively small oscillator strengths between the ground and first excited states. As a result of excitation from the first excited state to higher-lying electronic states that have faster intersystem crossing times, in typical photoinitiators the deactivation beam would enhance polymerization as opposed to inhibiting it.

To solve the oscillator strength problem, we searched for molecules with large absorption cross sections that are not typically used as radical photoinitiators but that can still generate radicals upon photoexcitation. We focused our search on molecules with a low fluorescence quantum yield, on the premise that a nonradiative process might lead to radical generation. We identified a number of such dyes that could act as photoinitiators for MAP (*16*). We then investigated whether a second laser beam could be used to deactivate any of these molecules after the initial excitation. We employed two tunable, synchronized Ti:sapphire lasers for these experiments. The excitation laser produced pulses of 200-fs duration centered at 800 nm (*16*). Continuous-wave (CW) radiation from the same laser did not lead to polymerization with any of the dyes tested, which verified that photoinitiation occurred through multiphoton absorption. The output of the second laser was stretched to a duration of ~50 ps to enhance the effectiveness of the stimulated emission process by allowing time for vibrational relaxation in the electronic ground state (*11*) and was tuned over a range of wavelengths to search for evidence of deactivation.

For one of the dye molecules tested, malachite green carbinol base, we were able to use the deactivation beam to reduce polymerization or, at high enough intensity, to inhibit polymerization completely (Fig. 1). We examined deactivation beam wavelengths ranging from 760 nm to 840 nm and in all cases were able to inhibit polymerization. The capacity to initiate polymerization with femtosecond pulses and inhibit polymerization with considerably longer pulses of the same wavelength confers the advantage that the entire process can be accomplished with the output of a single ultrafast laser if desired.

To demonstrate photoinduced deactivation of polymerization, we fabricated polymer lines with excitation and deactivation beams that were either offset or spatially coincident (Fig. 1A). Shown in Fig. 1B are lines drawn with an offset between the beams. The deactivation beam was blocked at regular periods with an optical chopper wheel. The resultant modulation of the polymer line demonstrates the effectiveness of the deactivation process.

In Fig. 1C, we show lines drawn by scanning the sample stage at constant velocity with no deactivation beam (lowest line) and with different timings between the excitation and deactivation pulses. The deactivation beam was set at an intensity that resulted in only partial inhibition of polymerization so that the dependence of the deactivation efficiency on timing could be determined. The efficiency of deactivation did not change noticeably for excitation/deactivation delays between 0 and 13 ns (*17*). This result implies that the photoinitiator goes through an intermediate state between optical excitation and the initiation of polymerization. The lifetime of this intermediate state must be considerably longer than 13 ns, making it likely that the state is deactivated through a process other than stimulated emission. Once a structure was polymerized, it could not be erased by subsequent application of the deactivation beam, indicating that for deactivation to be effective it must occur while the dye molecule is in this intermediate state. However, a region in which deactivation was used to prevent polymerization can be polymerized subsequently by the excitation beam.

Given the high peak intensity of the short excitation pulses, two-photon initiation dominates over one-photon deactivation when they impinge on the prepolymer resin. In contrast, 50-ps deactivation pulses have considerably greater duration and correspondingly weaker peak intensity, so their overall energy can be much greater than that of the excitation beam without causing polymerization. Thus, for these longer pulses, deactivation can dominate over initiation. Even with 50 ps pulses, at high enough average power the deactivation beam caused increased polymerization, presumably through two-photon absorption. Based on the observation that delays as long as 13 ns did not affect the deactivation efficiency, we tested whether deactivation could be driven by CW radiation, for which considerably higher deactivation intensities would be feasible. As shown in Fig. 1D for spatially coincident excitation and deactivation beams (with the latter beam chopped), CW radiation is indeed effective for deactivation. This result is important because it allows RAPID to be performed without the need to establish any timing between the excitation and deactivation lasers and also implies that RAPID lithography should be feasible with single-photon absorption using CW excitation and deactivation beams.

Figure 1B gives a clear indication of how using different spatial intensity patterns for these two beams can improve resolution. We therefore next explored spatial phase shaping of the deactivation beam to alter its intensity distribution in the focal region. Our experimental setup for RAPID lithography with a pulsed excitation beam and a phase-shaped, CW deactivation beam is shown in Fig. 2. This setup employs two Ti:sapphire lasers tuned to 800 nm, one operating in pulsed mode for multiphoton excitation and one operating in CW mode for deactivation. The outputs of the two lasers were set to orthogonal polarizations and combined in a polarizing beam cube. The beams were focused into the sample with a high-numerical-aperture objective, the back aperture of which was overfilled by the excitation beam and filled completely by the deactivation beam.

We employed a spatial phase mask (*11*) that is designed to improve resolution along the optical axis of the fabrication system, which we will designate *z*. The mask consists of a flat substrate with a central circular region of an appropriate thickness to create a half-wave delay at 800 nm. The point-spread functions (PSFs) of the two beams (*18*) were measured, and proper overlap

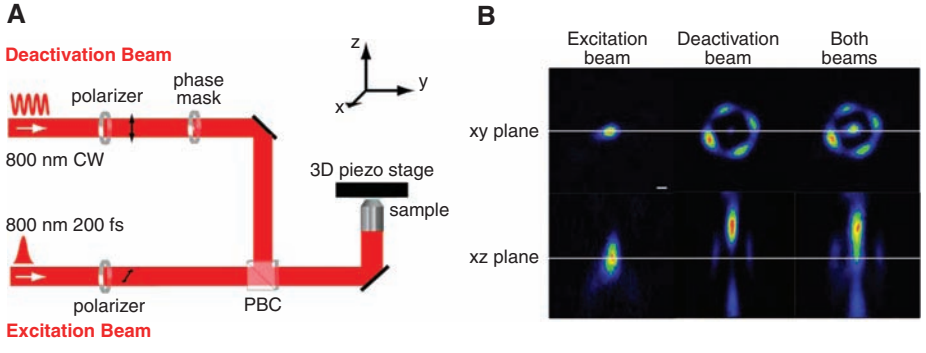

Fig. 2. (**A**) Schematic experimental setup for RAPID lithography with a pulsed excitation beam and a phase-shaped, CW deactivation beam. PBC, polarizing beam cube. (**B**) False-color, multiphoton-absorption–induced luminescence images of the cubes of the PSFs of the excitation beam, the deactivation beam, and both beams together. The long white lines indicate the approximate centers of the focal regions. The scale bar in the upper left image is 200 nm.

was ensured using multiphoton-absorption–induced luminescence (MAIL) (*19*) from a gold nanoparticle (Fig. 2B) (*20*). The majority of the intensity of the deactivation beam lies outside the center of the focal region. As can be seen from these images, there is no overlap between the excitation and deactivation PSFs in the *xy* plane, but there is considerable overlap along the *z* direction.

To assess the resolution enhancement of RAPID lithography with this phase mask, we studied the sizes and shapes of voxels created with different excitation and deactivation powers. To observe the voxel shapes, we employed an ascending-scan method in which identical, isolated voxels are created at different heights relative to the substrate (*10*). At some particular height, the voxel will barely be attached to the substrate. If the aspect ratio of the voxel is greater than unity it will fall over, allowing its dimensions to be determined readily with scanning electron microscopy (SEM) or atomic force microscopy (AFM).

Figure 3 shows SEM images from one such voxel study at a fixed excitation power (time averaged) of 10 mW (*21*) and different deactivation beam powers. As would be expected for the phase mask employed, deactivation did not have a substantial effect on the transverse dimensions of the voxels. However, with increasing deactivation power the *z* dimension of the voxel decreased by a factor of more than three. For a given excitation intensity, deactivation intensity, and height relative to the substrate, voxels were either present at every exposed spot or were absent at every exposed spot. The variation in voxel dimensions for a fixed set of fabrication parameters was about ±5%.

Because our voxel studies were performed on a glass cover slip (which is transparent but not electrically conductive), voxels had to be coated with metal for SEM imaging. Thus, to measure the smallest voxels that could be fabricated, we used AFM so that the metal coating step could be avoided. Shown in Fig. 3G is the smallest voxel that we were able to fabricate reproducibly with RAPID lithography using 800 nm light (*22*). For comparison, the corresponding smallest voxel that could be fabricated reproducibly without the deactivation beam is shown in Fig. 3H (*23*). Whereas the voxel in Fig. 3G is standing, the voxel in Fig. 3H has fallen over because of its high aspect ratio.

Resins used for MAP often exhibit shrinkage. The resin used here is composed of low-molecular-weight monomers that exhibit low shrinkage. To determine whether shrinkage takes on an increased importance at small feature sizes, we fabricated suspended polymer lines (fig. S1) with cross-sectional dimensions similar to those of the voxels in Fig. 3, G and H. The widths of the lines did not increase substantially at their attachment points to the supporting structures, and the lines are not always taut, which indicates that shrinkage is not responsible for the small voxel sizes observed here.

In Fig. 3I, we plot the height and aspect ratio of voxels measured in AFM experiments as a function of deactivation power. When the aspect ratio of a voxel is less than unity, it will not fall over even when barely attached to the substrate. For the excitation power used in Fig. 3I, we were able to reduce the voxel height from nearly 600 nm with no deactivation beam to 40 nm with a deactivation power of 93 mW, representing a resolution of λ/20. The aspect ratio was correspondingly reduced from more than 3 to 0.5. The rings on the towers shown in Fig. 3J (fabricated with conventional MAP) and Fig. 3K (fabricated with RAPID) demonstrate that enhancement of resolution and aspect ratio can also be achieved in 3D structures.

We have observed that above a certain excitation power, it becomes impossible to inhibit polymerization fully even at high deactivation beam power. This result implies that there are two different channels for photoinitiation, only one of which is deactivatable. If the concentration of radicals from the nondeactivatable channel is below the polymerization threshold, the deactivation beam can inhibit polymerization completely. We have further observed that the irreversible channel is weaker in more viscous resins. Although research into the nature of the photophysics of this system is ongoing, we believe that excitation of the photoinitiator leads to an electron transfer process that creates two relatively stable radicals. Due to their stability, these radicals initiate polymerization on a time scale

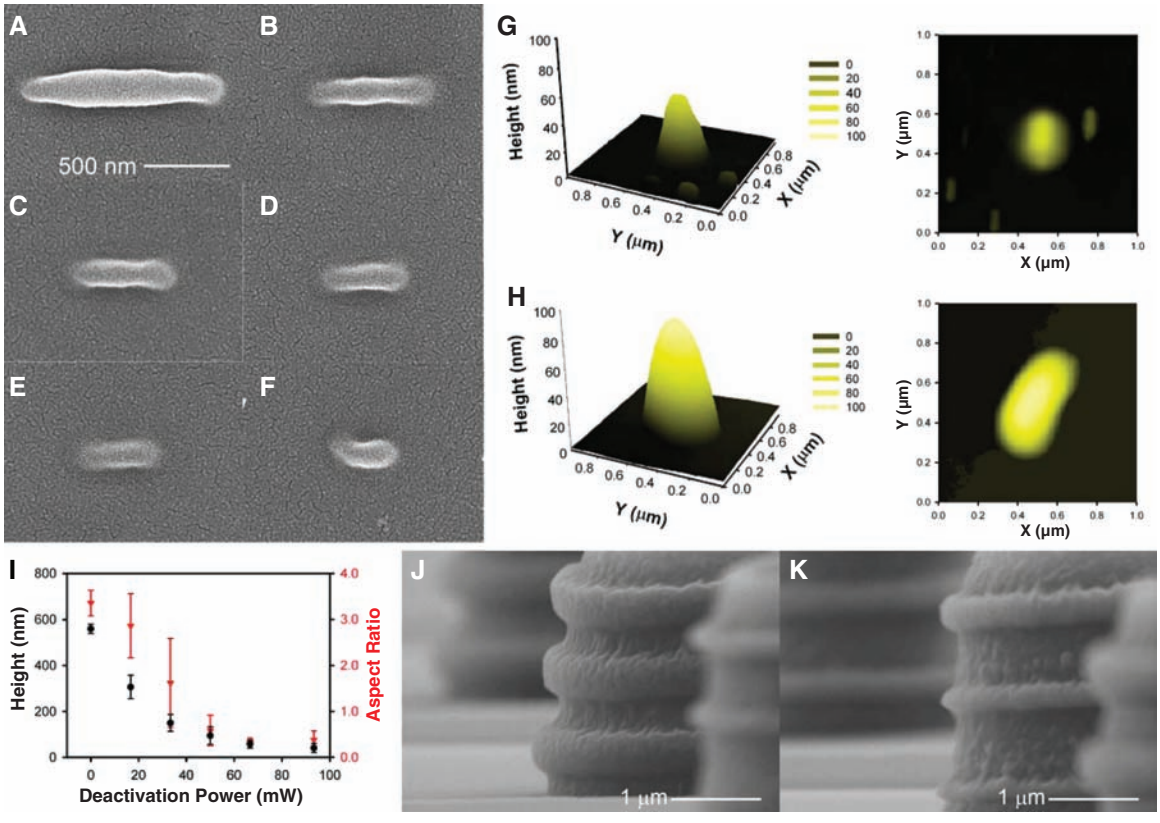

Fig. 3. (**A** to **F**) SEM images of voxels created with deactivation beam powers of 0 mW, 17 mW, 34 mW, 50 mW, 84 mW, and 100 mW, respectively. (**G**) Three-dimensional and contour AFM images of the smallest voxel that could be created with RAPID lithography. (**H**) Corresponding images of the smallest voxel that could be created with conventional MAP. The *x* and *y* dimensions of the voxels in (G) and (H) are exaggerated due to the width of the AFM tip, whereas the *z* dimension (height) is accurate. (**I**) Dependence of the height and aspect ratio of voxels on the power of the deactivation beam. The error bars represent ±1 SD based on measurements of four voxels. (**J**) Tower with rings created with conventional MAP. (**K**) Tower with rings created with RAPID.

that is considerably longer than the 13-ns repetition time of our laser system. So long as the radicals do not diffuse apart, absorption of a photon from the deactivation beam can lead to back-transfer of the electron, depleting the radicals before they can react. If the radicals do diffuse apart, deactivation can no longer occur, accounting for the nondeactivatable channel.

With the phase mask used here, RAPID lithography can clearly produce features with heights as small as λ/20 along the optical axis. Analogous with results from STED microscopy, comparable transverse resolution should be attainable by employing a different phase mask, such as a spiral phase element (*24*). By using two phase-masked deactivation beams (*25*), it should further be possible to attain this resolution in all dimensions. The use of shorter excitation and deactivation wavelengths should improve resolution further. A current limiting factor in the resolution attainable is that even a CW deactivation beam can cause polymerization at high enough intensity. Because the resolution enhancement of RAPID lithography is based on an optical saturation effect, making the deactivation process more efficient should lead to finer features. In principle, the resolution of RAPID will ultimately be limited by material properties, particularly the minimum size of a self-supporting polymer voxel. With this limitation in mind, we believe that resolution on the order of 10 nm can be attained through full optimization of the photoresist properties and the optical configuration. Resolution on this scale may be attractive for next-generation lithography, particularly considering that RAPID lithography can be implemented with a table-top instrument.

References and Notes

1. S. E. Thompson, S. Parthasarathy, *Mater. Today* **9**, 20 (2006).
2. H. Ito, in *Microlithography: Molecular Imprinting* (Springer-Verlag, Berlin, 2005), vol. 172, *Advances in Polymer Science*, pp. 37–245.
3. S. Kawata, H. B. Sun, T. Tanaka, K. Takada, *Nature* **412**, 697 (2001).
4. M. Rumi, S. Barlow, J. Wang, J. W. Perry, S. R. Marder, in *Photoresponsive Polymers I* (Springer-Verlag, Berlin, 2008), vol. 213, *Advances in Polymer Science*, pp. 1–95.
5. C. N. LaFratta, J. T. Fourkas, T. Baldacchini, R. A. Farrer, *Angew. Chem. Int. Ed.* **46**, 6238 (2007).
6. D. Yang, S. J. Jhaveri, C. K. Ober, *Mater. Res. Sci. Bull.* **30**, 976 (2005).
7. J.-F. Xing *et al.*, *Appl. Phys. Lett.* **90**, 131106 (2007).
8. D. Tan *et al.*, *Appl. Phys. Lett.* **90**, 071106 (2007).
9. W. Haske *et al.*, *Opt. Express* **15**, 3426 (2007).
10. H.-B. Sun, T. Tanaka, S. Kawata, *Appl. Phys. Lett.* **80**, 3673 (2002).
11. T. A. Klar, S. Jakobs, M. Dyba, A. Egner, S. W. Hell, *Proc. Natl. Acad. Sci. U.S.A.* **97**, 8206 (2000).
12. S. W. Hell, *Science* **316**, 1153 (2007).
13. S. W. Hell, *Nat. Methods* **6**, 24 (2009).
14. C. S. Colley *et al.*, *J. Am. Chem. Soc.* **124**, 14952 (2002).
15. J. O. Hirschfelder, C. F. Curtiss, R. B. Bird, *Molecular Theory of Gases and Liquids* (Wiley, New York, 1954).
16. Materials and methods are available as supporting material on *Science* Online.
17. The maximum delay time of 13 ns is determined by the 76 MHz laser repetition rate.
18. Because MAIL from gold nanoparticles is a three-photon process at 800 nm, the images show the cubes of the PSFs.
19. R. A. Farrer, F. L. Butterfield, V. W. Chen, J. T. Fourkas, *Nano Lett.* **5**, 1139 (2005).
20. The deactivation laser was operated in fs pulsed mode for the purpose of measuring its PSF using MAIL but was operated in CW mode for all other experiments. The beam profile and direction did not change measurably in going from pulsed to CW mode, so we expect the PSF to be nearly identical in both modes.
21. All powers were as measured at the sample position.
22. The slight asymmetry of the voxel is due to our use of linearly polarized light for fabrication. See (*26*).
23. AFM cannot measure reentrant (overhanging) features, so although the voxels appear to be tapered in these images, they are not.
24. M. W. Beijersbergen, R. P. C. Coerwinkel, M. Kristensen, J. P. Woerdman, *Opt. Commun.* **112**, 321 (1994).
25. B. Harke, C. K. Ullal, J. Keller, S. W. Hell, *Nano Lett.* **8**, 1309 (2008).
26. H. B. Sun *et al.*, *Appl. Phys. Lett.* **83**, 819 (2003).

27. We appreciate the support of the Maryland NanoCenter and its Nanoscale Imaging, Spectroscopy, and Properties Laboratory (NISPLab). NISPLab is supported in part by NSF as a *Materials Research Science and Engineering Center* (MRSEC) Shared Experimental Facility. This work was supported in part by the UMD-NSF-MRSEC under grant DMR 05-20471. We are grateful to E. Williams for the use of her AFM and to J. Goldhar, Y. Leng, and V. Yun for fabricating the phase mask used in this work. The University of Maryland has filed a provision patent based on the work presented in this paper.

Supporting Online Material

www.sciencemag/org/cgi/content/full/1168996/DC1
Materials and Methods
SOM Text
Fig. S1
References

25 November 2008; accepted 19 March 2009
Published online 9 April 2009;
10.1126/science.1168996
Include this information when citing this paper.

Two-Color Single-Photon Photoinitiation and Photoinhibition for Subdiffraction Photolithography

Timothy F. Scott,[1]* Benjamin A. Kowalski,[2] Amy C. Sullivan,[2]† Christopher N. Bowman,[1] Robert R. McLeod[2]‡

Controlling and reducing the developed region initiated by photoexposure is one of the fundamental goals of optical lithography. Here, we demonstrate a two-color irradiation scheme whereby initiating species are generated by single-photon absorption at one wavelength while inhibiting species are generated by single-photon absorption at a second, independent wavelength. Co-irradiation at the second wavelength thus reduces the polymerization rate, delaying gelation of the material and facilitating enhanced spatial control over the polymerization. Appropriate overlapping of the two beams produces structures with both feature sizes and monomer conversions otherwise unobtainable with use of single- or two-photon absorption photopolymerization. Additionally, the generated inhibiting species rapidly recombine when irradiation with the second wavelength ceases, allowing for fast sequential exposures not limited by memory effects in the material and thus enabling fabrication of complex two- or three-dimensional structures.

Photopolymerizations typically proceed when a chromophore absorbs a photon and subsequently generates active centers that initiate the polymerization reaction. This single-photon process exhibits high irradiation sensitivity, enabling the use of low-power lasers and high writing speeds, which are critical for lithographic, stereolithographic, and data storage applications. However, feature size in depth is typically a multiple of the Rayleigh range of the focused beam (*1*), preventing the fabrication of micrometer-scale layers. Similarly, the transverse feature size is constrained by the diffraction limit, a physical property associated with the focusing power of lenses that is dependent on the wavelength of the incident light and the numerical aperture of the lens. Finer feature sizes are achieved by reducing the irradiation intensity or time (*2*); however, this procedure unavoidably reduces the contrast between the conversion of the gelled, insoluble material and the ungelled, soluble material and results in the fabrication of loosely cross-linked, mechanically unsound structures unable to withstand the rigors of solvent processing that are necessary for device fabrication.

These limitations are partially addressed by two-photon photopolymerization, wherein a chromophore absorbs two photons to initiate polymerization. This approach has been exploited by a number of researchers to realize the fabrication of three-dimensional (3D) nanostructures (*2*–*6*) with

[1]Department of Chemical and Biological Engineering, University of Colorado, Boulder, CO 80309–0424, USA. [2]Department of Electrical and Computer Engineering, University of Colorado, Boulder, CO 80309–0425, USA.

*Present address: Center for Bioengineering, Department of Mechanical Engineering, University of Colorado, Boulder, CO 80309–0427, USA.

†Present address: Department of Physics and Astronomy, Agnes Scott College, Decatur, GA 30030, USA.

‡To whom correspondence should be addressed. E-mail: robert.mcleod@colorado.edu